

## Detection of adsorption sites at the gap of a hetero-metal nano-dimer at the single molecule level

Mai Takase, Yoshitaka Sawai, Hideki Nabika, Kei Murakoshi\*

Department of Chemistry, Faculty of Science, Hokkaido University, Sapporo 060-0810, Japan

### ARTICLE INFO

#### Article history:

Available online 30 March 2011

#### Keywords:

Surface-enhanced Raman scattering  
Heterometal nanodimer  
Single molecule spectroscopy  
Adsorption site

### ABSTRACT

*In situ* surface-enhanced Raman scattering (SERS) measurements were carried out using Au homo, Ag homo and Au–Ag hetero-dimer structures with controlled gap distances. Controlled adsorption of 2,2'-bipyridine and 4,4'-bipyridine molecules onto the surface of metals in an aqueous solution resulted in characteristic SERS peak shifts reflecting switching of the adsorption site at the gap of the Au–Ag hetero-dimer. Changes in the relative intensities and the wavenumbers of the SERS bands provided information on the adsorption environment of the target molecule at the single molecule level.

Crown Copyright © 2011 Published by Elsevier B.V. All rights reserved.

### 1. Introduction

Inspired by the pioneering works on the surface enhanced Raman scattering (SERS) phenomenon in the 1970s [1,2], numerous experimental and theoretical investigations have been carried out in order to gain insight into the physico-chemical mechanism of the SERS phenomenon [3–7]. Several findings of ultra-sensitive detection at the single molecule level [9,10] triggered a renewed interest in this field from both scientific and technological viewpoints. Growing activities in technological research have enabled not only *in vitro* but also *in vivo* SERS analysis [10–12].

Regarding the single molecule sensitivity of SERS, strong proof has been reported by using a bi-analyte technique, in which two spectrally distinguishable molecules were used in the SERS measurement [13–15]. Although the sample was prepared by mixing these bi-analyte molecules together in colloidal Ag solution, SERS signals were observed that were composed of purely one or the other type of molecule. This is clear evidence that the observed SERS signal originates from a very small number of molecules at a single SERS active site, since the probability of observing large numbers of the same molecule from a single site is as low as 1/32 for 5 molecules and 1/1024 for 10 molecules in the bi-analyte system. Similarly, our group has discovered by the bi-analyte technique that the SERS signal switched from one to the other type of molecule during successive observations [16], which is also strong evidence that only a single or a small number of molecules at single sites were being detected. Generally, SERS with single molecule sensi-

tivity is acquired when the molecule is situated at the gap between two adjacent gold or silver dots, since calculations based on electromagnetic theory predict that the electromagnetic field is confined to the gap region [17]. In addition to the theoretical prediction, the field confinement at the gap of the Au dimer has been experimentally visualized by using two-photon polymerization [18]. This showed that two-photon polymerization occurred only at the gap when the excitation light was linearly polarized along the long axis of the dimer, which supports the theoretical prediction for field confinement at the gap.

In order to explore potential applications of the SERS phenomenon, diverse kinds of gap or dimer structures have been employed, including dot arrays [16,18], colloidal aggregations [8,9,13], and dot–surface pairs [19,20]. In contrast to the dot array or colloidal aggregation systems which usually use Au or Ag homodimers or homo-aggregates, the dot–surface pair enables the construction of hetero-dimeric structures by choosing an appropriate dot to be adsorbed on the surface. For example, Park et al. have fabricated and compared two independent systems: Au dot–Au surface and Ag dot–Au surface pairs [19]. Their results demonstrated strong metal dependency in the spectral features of the SERS signal, which has been explained by taking into account the difference in Fermi energies of Au and Ag dots. This finding resulted from the fact that the SERS signal from single molecules contains information of their circumstances, e.g., the nearby material, local field anisotropy, local temperature, local ionic strength, etc. [21–23]. However, this type of information from hetero-dimeric systems has not been discussed in detail and is quite limited, especially in the dot array or colloidal aggregation systems, despite the fact that most SERS-based applications rely on them.

Herein, we investigate the spectral features of SERS from the dot array system with well-defined hetero-dimeric structures. Both

\* Corresponding author. Tel.: +81 11 706 2704; fax: +81 11 706 4810.  
E-mail address: [kei@sci.hokudai.ac.jp](mailto:kei@sci.hokudai.ac.jp) (K. Murakoshi).

homo- and hetero-dimer structures were fabricated by angle-resolved nanosphere lithography [24]. In this method, the dimer array is obtained by a successive deposition of metal while changing the deposition angle. Along with the change in the deposition angle, changing the metal for the first and the second depositions makes it possible to fabricate hetero-dimers composed of different metals. In the present study, we will compare the SERS signal from Au–Au and Ag–Ag homo-dimer systems and the Au–Ag hetero-dimer system.

## 2. Experimental

The detailed experimental procedures in the present study were described in our previous report [25].

The Au–Au, Ag–Ag, and Au–Ag dot dimer arrays were prepared by an angle-resolved nanosphere lithography technique (AR-NSL) using repeated vapor depositions with different angles onto the polystyrene (PS) particle (Polysciences Inc.; diameters were 200 nm for Au homo- and Au–Ag hetero-dimer systems and 350 nm for Ag homodimer system) monolayer prepared on a glass substrate. The aqueous PS particle suspension was concentrated to 8 and 10 wt.%, and then diluted by ethanol (60 and 50%). In addition to the previously documented drop-coating method, we adapted the method using PS monolayers prepared on liquid–gas interfaces to improve the quality of the array. The PS solutions (20  $\mu\text{L}$ ) were dropped onto the convex surface of a watch glass immersed in Milli-Q water. The thin water layer on the glass surface leads to uniform spreading of PS beads on the air–water interface. After the spreading of PS beads on the water surface, the layer was packed tightly over time. The change in the surface tension of the water around the PS layer results in the formation of well-ordered monolayers with low density of defects, dislocations, and vacancies on the liquid–water interface. The prepared high quality monolayer was then lifted off from the water surface using a cleaned glass substrate. The metal was deposited onto the PS monolayer prepared on the glass substrate. After the first metal deposition, the second metal was deposited with different angles. Then, the PS mask was removed by sonication in Milli-Q water for 10–30 s. The extinction spectra of the metal dimer array in the visible–near infrared region were recorded using a multi-channel spectrometer (MCPD-2000, Ohtsuka Electronics). The structure of the dimer on the glass substrate was inspected by an atomic force microscope (AFM, Nanoscope-IIIa, Digital Instruments) in air.

A commercial Raman microprobe spectrometer (Ramanscope System-2000, Renishaw) was specially modified for NIR laser light ( $\lambda_{\text{ex}} = 785 \text{ nm}$ ). The expanded NIR beam is focused onto the sample using a water-immersion objective lens with 100 $\times$  magnification and a numerical aperture of 1.0. The estimated spot size of irradiation was ca. 1  $\mu\text{m}$ , with tunable output intensity in the range between 30  $\mu\text{W}$  (3.8  $\text{kW cm}^{-2}$ ) and 200  $\mu\text{W}$  (25.5  $\text{kW cm}^{-2}$ ). All Raman measurements were carried out *in situ* by immersion of the SERS active substrates into aqueous solutions containing the target molecules (2,2'-bipyridine, 4,4'-bipyridine; reagent grade, Wako Co. Ltd.) at controlled concentrations (1, 10 and 100  $\mu\text{M}$ ).

## 3. Results and discussion

Optical properties of the metal dimers were optimized for the SERS measurements using the 785 nm (1.58 eV) light excitation. The Au-homodimer and the Ag-homodimer were prepared by the evaporation angles of  $-11^\circ/+11^\circ$  and  $0^\circ/+24^\circ$ , respectively, which were optimized in the previous reports [16,25]. For the Au–Ag hetero-dimer, the deposition angles were  $0^\circ/+24^\circ$ . Fig. 1 shows the extinction spectra of the metal dimer arrays measured by the

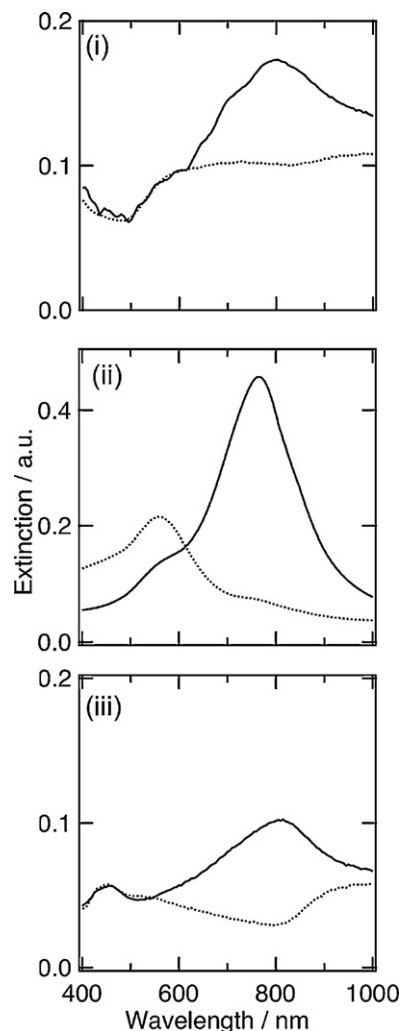


**Fig. 1.** Polarized extinction spectra of (i) Au-homodimer, (ii) Ag-homodimer, and (iii) Au–Ag hetero-dimer. Polarization angles to the long axis  $\theta$  were  $0^\circ$  (solid line) and  $90^\circ$  (dotted line).

polarized incident light. These extinction spectra were found to be independent of the observed area within ca. 0.3  $\text{cm}^2$ . This result indicates the successful preparation of uniform and well-ordered structures of the metal dimer array with relatively large areas. The polarized excitation along the long axis of the dimers led to the appearance of a peak at longer wavelengths around 800 nm. When the polarization of the illuminated light was aligned with the short axis of the metal dimers, the peaks around 800 nm disappeared. This apparent dependence of the polarization direction on structural anisotropy of the dimer suggests successful excitation of the localized surface plasmon modes of the respective metal dimer structures in the present system.

Fig. 2 presents typical AFM images of the Au–Ag hetero-dimer structure. The size of the perpendicular bisectors of the equilateral Au triangles formed by the first deposition was approximately 60 nm, and the diameter of the Ag dot formed by the second deposition was approximately 20 nm (Fig. 2(a)). Directions of the long axis of the individual dimers were well aligned with the azimuth of the second deposition (Fig. 2(b)).

Relatively intense SERS was observed from the substrates with the metal dimers immersed in aqueous solution containing 2,2'-bipyridine and 4,4'-bipyridine. Fig. 3(a) shows the SERS spectra measured using the Au-homo, the Ag-homo, and the Au–Ag hetero dimers, immersed in an aqueous solution containing 100  $\mu\text{M}$

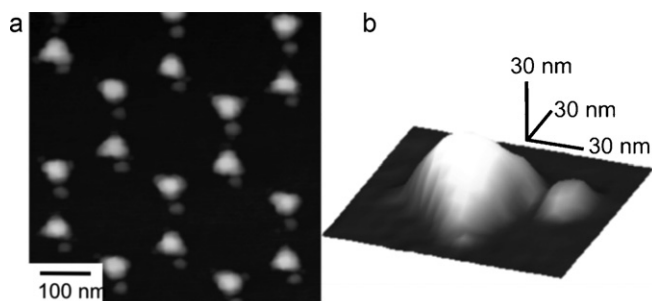


Fig. 2. (a) Two-dimensional and (b) three-dimensional AFM images of Au-Ag hetero-dimer.

2,2'-bipyridine. Observed SERS bands are attributable to the vibrational modes of the ring breathing around  $1016\text{ cm}^{-1}$ , the in-plane ring deformation coupled with the C-H bending at  $1060\text{ cm}^{-1}$ , and the inter-ring stretching at  $1300\text{ cm}^{-1}$  [26]. The expanded plot of the SERS spectra around  $980\text{--}1040\text{ cm}^{-1}$  shows that the  $1012\text{--}1016\text{ cm}^{-1}$  band of the ring breathing mode observed at the Au-homo dimer (Fig. 3(a, i)) shifts to  $1008\text{--}1012\text{ cm}^{-1}$  in the sys-

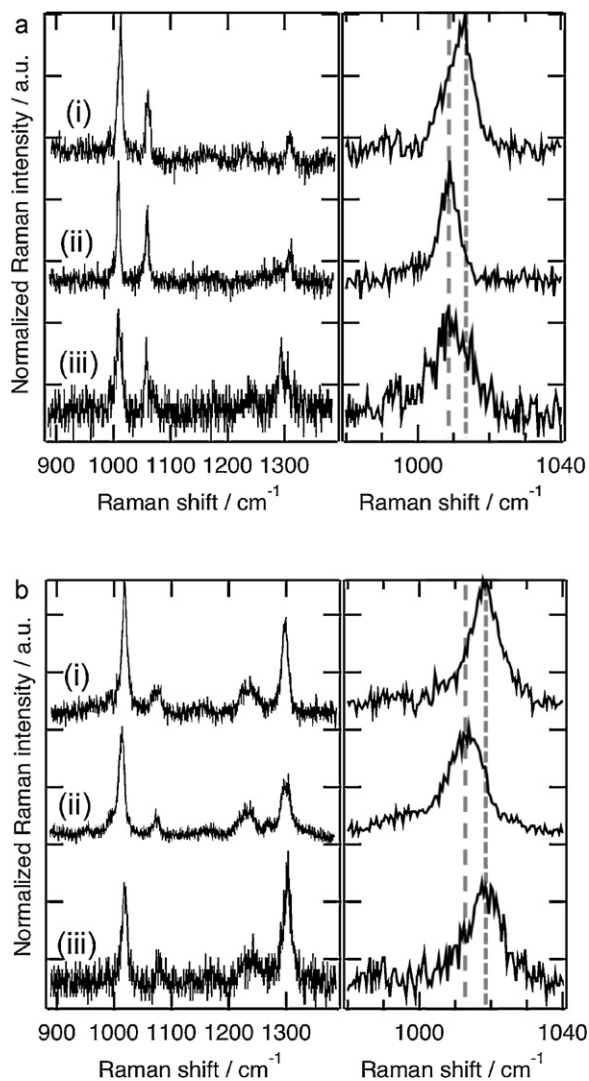


Fig. 3. SERS spectra of (a) 2,2'-bipyridine and (b) 4,4'-bipyridine. The substrates were (i) Au-homodimer, (ii) Ag-homodimer, and (iii) Au-Ag hetero-dimer. Each spectrum was acquired in  $100\text{ }\mu\text{M}$  bipyridine solution. The excitation laser power was  $25.5\text{ kW cm}^{-2}$  and the exposure time was 1 s.

tem of the Ag-homo dimer (Fig. 3(a, ii)). This difference in the wavenumber of the ring breathing mode may reflect the change in the electron density of the ring due to the difference in the adsorption strength of 2,2'-bipyridine molecules on the surface of the Au-homo and the Ag-homo dimers. It is noteworthy that the ring breathing observed at the Au-Ag hetero dimer gives a broad peak centered around  $1012\text{ cm}^{-1}$ . The vibrational band of the ring breathing mode in the SERS spectrum of the Au-Ag hetero dimer seems to be superimposed on those observed at the Au-homo and the Ag-homodimers.

Quite similar changes in the wavenumber of the ring breathing mode in the metal dimers were also observed in an aqueous solution of 4,4'-bipyridine. Fig. 3(b) shows SERS spectra of 4,4'-bipyridine with the metal dimers. The vibration modes are assigned to the ring breathing around  $1020\text{ cm}^{-1}$ , the in-plane ring deformation coupled with the C-H bending at  $1080\text{ cm}^{-1}$ , the in-plane C-H bending at  $1240\text{ cm}^{-1}$  and the inter-ring stretching at  $1300\text{ cm}^{-1}$  [27,28]. The ring breathing mode observed at the Au-homodimer ( $1018\text{ cm}^{-1}$ ) was at a higher wavenumber than that for the Ag-homodimer ( $1015\text{ cm}^{-1}$ ). The band at the Au-Ag hetero-dimer was slightly broadened around  $1018\text{ cm}^{-1}$  comparable to the Au-homo dimer.

In our previous report, we proved that relatively intense SERS originates from the gap part of the dimer with optimized structure for effective localized surface plasmon excitation. *In situ* SERS measurements using a system with a controlled surface coverage of bi-analyte suggest that the SERS active sites are comparable in size to a single molecule [16]. The present systems were comparable to those in the previous report, i.e., the surface coverage of adsorbed molecules is less than one monolayer on the metal surfaces. Thus, SERS spectra observed in the present system may reflect the information on the adsorption site at a single molecule level.

The wavenumber of the ring breathing mode at the Au-Ag hetero-dimer showed characteristic behavior of a time-dependent change. In Fig. 4, SERS spectra sequentially recorded every 1 s are shown using the Au-Ag hetero-dimer in  $100\text{ }\mu\text{M}$  2,2'-bipyridine solution. Although relative intensities of the respective bands are rather stable, the spectral features of the ring breathing mode indicate time-dependent changes. A broad band at  $t=7\text{ s}$  and  $8\text{ s}$  became sharp at  $t=9\text{ s}$  with a peak at  $1010\text{ cm}^{-1}$ . The peak shifts to  $1016\text{ cm}^{-1}$  while remaining sharp at  $t=10\text{ s}$ . The peak broadens again after  $t=11\text{ s}$ . These observed time-dependent changes of the band feature reflect the adsorption site at the gap of the Au-Ag hetero dimer at the single molecule level. The intensity of the peak was deconvoluted to estimate the possibility of adsorption on the Au and Ag surface based on the difference in the wavenumbers of the ring breathing mode at Au and Ag. Fig. 4(b) shows the time course of the relative ratio of SERS intensities from 2,2'-bipyridine molecules on Au to those on the Ag surface. A value of 0.5 corresponds to the possibility of equal adsorption on the Au and Ag surfaces. Changes in the spectral feature at  $t=9\text{ s}$  and  $10\text{ s}$  are successful observations of the adsorption site of 2,2'-bipyridine switching from the Ag to the Au surface at the gap of the Au-Ag hetero dimer. The significant change in the values of the ratio from zero to unity suggests that the number of observed molecules is quite small. Values between 0.2 and 0.4 before and after the site switching indicate that the possibility of adsorbing on Ag is slightly higher than that on Au. These results also suggest that the time scale of the site switching should be on the order of a second. However, this adsorption time was limited when the single molecule was at the same metal dot during 1 s of Raman exposure time. If molecular adsorption time is shorter than 1 s, we will observe a spectral change in Fig. 4 when molecular switching is on the same metal structure.

A time-dependent change in the feature of the ring breathing mode was also observed in  $10\text{ }\mu\text{M}$  4,4'-bipyridine solution (Fig. 5). Although the site switching behavior between Au and Ag was not

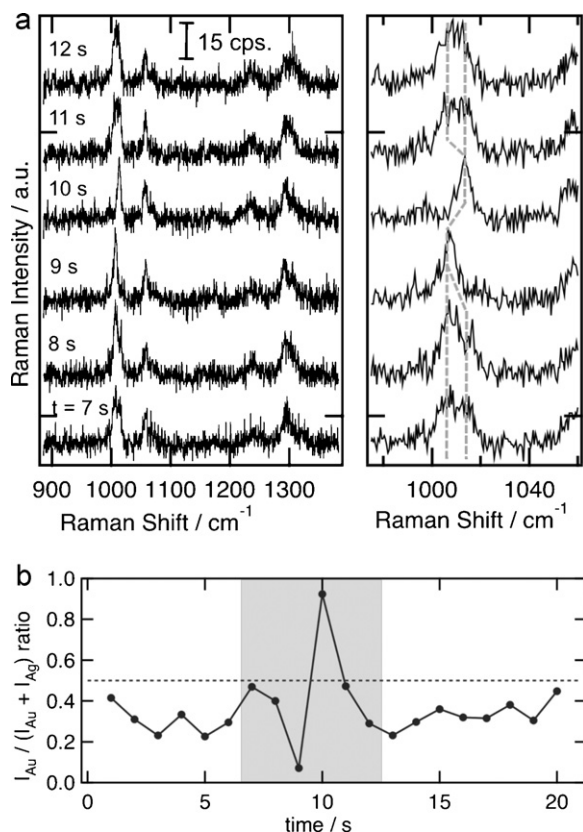


**Fig. 4.** (a) Successive SERS spectra of 2,2'-bipyridine on Au-Ag hetero-dimer substrate and (b) time course of SERS intensity of the ring breathing mode. The grey region in (b) indicates the time for SERS measurements shown in (a).

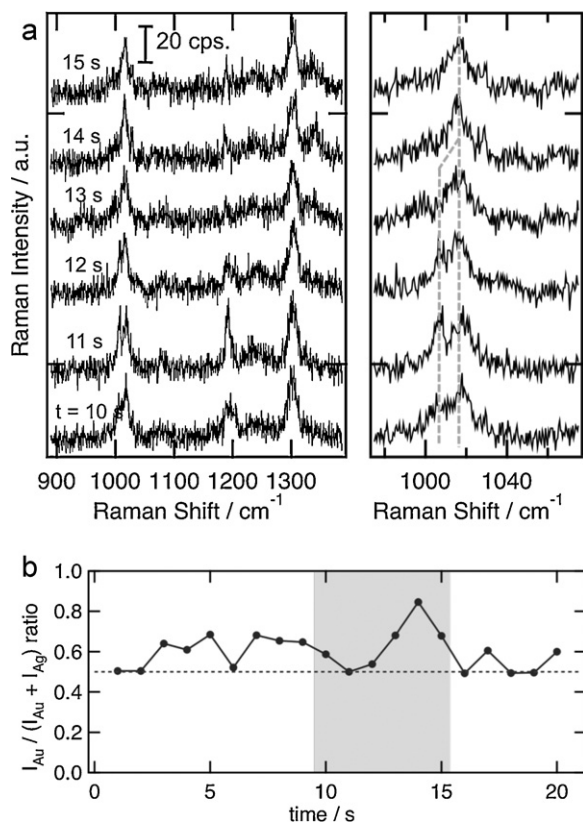


**Fig. 5.** (a) Successive SERS spectra of 4,4'-bipyridine on Au-Ag hetero-dimer substrate and (b) time course of SERS intensity of the ring breathing mode. The grey region in (b) indicates the time for SERS measurements shown in (a).

as apparent as in the case of 2,2'-bipyridine, a relatively sharp peak at higher wavenumber ( $1018\text{ cm}^{-1}$ ) was observed as the adsorption on Au at  $t = 14\text{ s}$  (Fig. 5(a)). A time course value of the relative intensity ratio of slightly larger than 0.5 implies that adsorption of 4,4'-bipyridine is rather stable, reflecting stronger adsorption on Au than Ag. A characteristic feature of the ring breathing band of 4,4'-bipyridine at the Au-Ag hetero-dimer is a narrower band width than that of 2,2'-bipyridine. Even when the value is 0.5, two sharp peaks are observed in the SERS spectrum, especially at  $t = 11\text{ s}$ . This characteristic feature of the sharp spectra should reflect well-defined states of the adsorption of 4,4'-bipyridine at the gap of the Au-Ag hetero-dimer. Another sharp peak at  $1020\text{ cm}^{-1}$  associated with the sharp peak of the ring breathing mode ( $t = 11\text{ s}$ ) could be correlated with the adsorption structure as discussed later.

The coverage of bipyridine molecules adsorbed on metal surfaces can be controlled by changing the concentration of molecules in solution. The adsorption isotherm indicates that increments from  $1\text{ }\mu\text{M}$  to  $100\text{ }\mu\text{M}$  correspond to the change of the coverage from less than 10% to full coverage [29,30]. The concentration dependence of the relative ratio of the SERS intensities of molecules on Au and Ag was investigated to evaluate the effect of the surface coverage on the adsorption orientation. Fig. 6 shows histograms of the relative ratio observed in  $1\text{ }\mu\text{M}$ ,  $10\text{ }\mu\text{M}$ , and  $100\text{ }\mu\text{M}$  solutions. In 2,2'-bipyridine solution (Fig. 6(a)–(c)), the maximum of the relative ratio shifts from 0.5 to 0.4 as the concentration changes from  $1\text{ }\mu\text{M}$  to  $100\text{ }\mu\text{M}$ . This result indicates that the possibility of adsorbing on Ag becomes higher as the surface coverage of 2,2'-bipyridine increases. The shift of the maximum was not observed in 4,4'-bipyridine as shown in Fig. 6(d) and (e). The most probable relative ratio is approximately 0.5 in these concentration ranges. Distri-

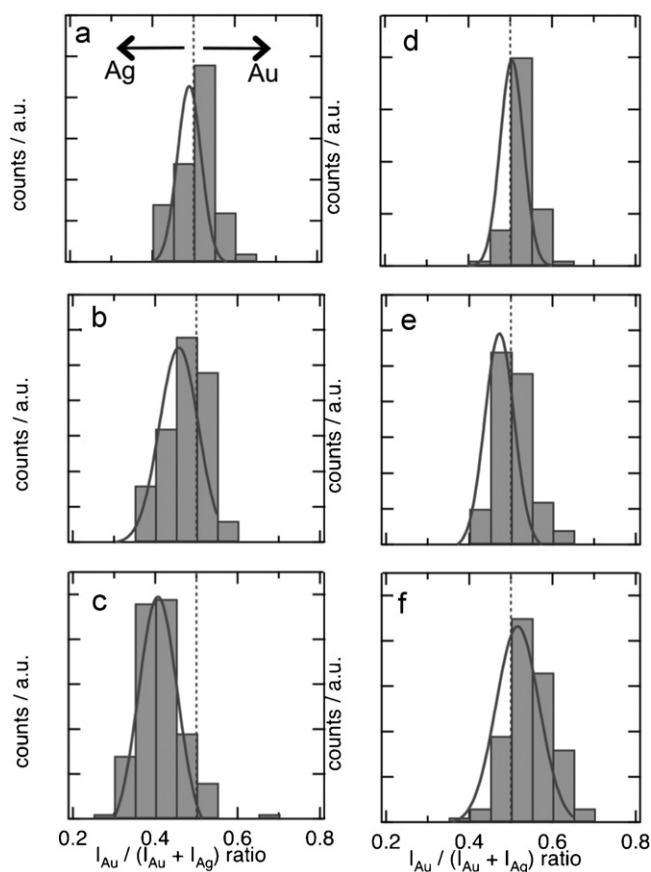


**Fig. 6.** Histograms of  $I_{\text{Au}}/(I_{\text{Au}} + I_{\text{Ag}})$  for (a–c) 2,2'-bipyridine and (d–f) 4,4'-bipyridine systems. The Bipyridine concentrations are (a and d)  $1\text{ }\mu\text{M}$ , (b and e)  $10\text{ }\mu\text{M}$ , and (c and f)  $100\text{ }\mu\text{M}$ .

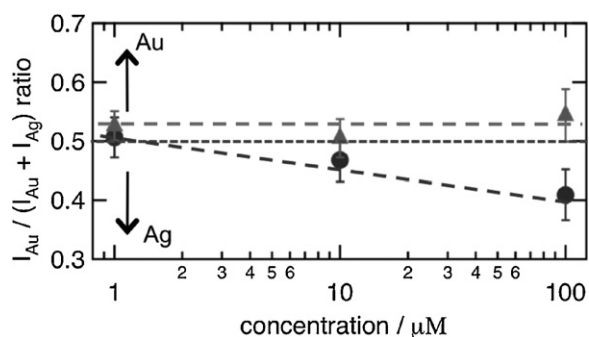


Fig. 7. Averaged  $I_{\text{Au}}/(I_{\text{Au}} + I_{\text{Ag}})$  of (●) 2,2'-bipyridine and (▲) 4,4'-bipyridine as the function of bipyridine concentration.

bution of the histogram broadens as the concentration increases, suggesting that the adsorption states of 4,4'-bipyridine at the gap of the Au–Ag dimer are not affected significantly by the change in the surface coverage. These characteristics of the relative ratio as a function of bipyridine concentration are summarized in Fig. 7.

Based on the change in the SERS spectral features of the ring breathing mode, we can discuss the states of the adsorbed molecules at the gap of the Au–Ag hetero dimer. The effect of the concentration on the switching behavior of 2,2'-bipyridine suggests a contribution of the intermolecular interaction to the strength of the adsorption and/or the SERS activity. The larger relative ratio due to the adsorption of 2,2'-bipyridine on Ag at 100  $\mu\text{M}$  implies that full coverage of the molecules on the metal surface results in stronger SERS, reflecting relatively strong coordination of molecules on Ag compared with Au.

The difference in the concentration dependence of 4,4'-bipyridine could not be explained by the difference in the strength of the adsorption on Au and Ag. Estimated adsorption energies of 2,2'- and 4,4'-bipyridine on Au are 42  $\text{kJ mol}^{-1}$  and 35  $\text{kJ mol}^{-1}$ , respectively [29,30]. Although the adsorption energy of 4,4'-bipyridine is smaller than that of 2,2'-bipyridine, stronger molecular interaction between 4,4'-bipyridine molecules adsorbed on surfaces leads to higher coverage than 2,2'-bipyridine at comparable concentrations. These previously documented characteristics suggest a more sensitive response of 4,4'-bipyridine than 2,2'-bipyridine. One of the possible factors which may cause the insensitive response of the relative intensity ratio of 4,4'-bipyridine on the solution concentration observed in the present system is the formation of a bridging structure at the gap between Au and Ag by the 4,4'-bipyridine molecule. Both ends of a 4,4'-bipyridine molecule adsorbed on Au and Ag may contribute to the observation of characteristic SERS band features of the ring breathing mode on Au and Ag. The bridging of the molecule at the gap should lead to restriction of the motion on the surface. Doubled sharp peaks shown in Fig. 5(a) at  $t = 11$  s could be considered as characteristic features of the bridging molecule. Another sharp peak simultaneously observed at 1018  $\text{cm}^{-1}$  is attributable to the ring breathing mode of 4,4'-bipyridine on the Au surface and is always observed. On the other hand, the peak at 1015  $\text{cm}^{-1}$  for the ring breathing mode at the Ag surface is not always observed. Also, the Raman signal of 4,4'-bipyridine on the Ag surface is not observed. In Fig. 5(a), the spectrum of 4,4'-bipyridine on the Ag surface was weaker than when the molecule was on the Au surface. Thus, if a molecule on the Ag surface is stronger than on the Au surface, what is observed is predicted if the number of molecules increases and absorbs to the Ag surface as well as to Au. Therefore, a molecule did not adsorb on each metal surface, but a molecule adsorbed only on the Au surface provided the spectrum on the Ag surface, i.e., 4,4'-bipyridine adopts a bridging structure between Au and Ag. Additionally, in the spectrum believed to be of the bridging structure, a new sig-

nal at 1200  $\text{cm}^{-1}$  was observed, and the possibility that this signal indicates a bridging structure has been suggested [31–34]. Generally, vibrational band at 1200  $\text{cm}^{-1}$  are not observed even at SERS measurements using homo Au–Au and Ag–Ag dimers as shown in Fig. 3. Relatively sharp and intense feature of 1200  $\text{cm}^{-1}$  band in the spectrum at  $t = 11$  s (Fig. 5) reflects very characteristics structure of the adsorbed molecule. In the system of the Au–Ag hetero dimer, bridging structure between Ag and Au at the gap of dimer should be the most probable structure. There is no other possible structure showing double peaks at 1018 and 1020  $\text{cm}^{-1}$  at the peak switching behavior. Broadening of the distribution in the histogram at higher concentration (Fig. 6(d)–(e)) may also reflect broadening of the adsorption due to the intermolecular interaction.

#### 4. Conclusions

We succeeded in preparing a SERS active Au–Ag hetero nanodimer structure showing SERS bands comparable to those observed at the Au and Ag homo-dimer structures. Adsorption orientation of 2,2'- or 4,4'-bipyridine molecules at the gaps of the Au–Ag hetero-dimer and Au or Ag homo-dimers were evaluated qualitatively based on analyses of relative intensities and wavenumbers of the SERS bands. When 2,2'-bipyridine molecule was used as the analyte, the switching of the adsorption site between different metals was observed in the change in the SERS spectra. In the case of 4,4'-bipyridine, a very characteristic feature of the SERS spectra was observed, suggesting the formation of a bridging structure at the gap of the Au–Ag hetero-dimer. The present Au–Ag hetero-dimer system may offer a model to obtain information on the adsorption site and orientation of a small number of molecules in ultra-small spaces.

#### Acknowledgments

This work was supported in part by Grants-in-Aid for Scientific Research Nos. 19049003 and 20750001, and from the Ministry of Education, Science and Culture, Japan. We are especially grateful for the Priority Area “Strong Photon-Molecule Coupling Fields (No. 470).” MT also thank to Grant-in-Aid for JSPS Fellows.

#### References

- [1] M. Fleischmann, P.J. Hendra, A.J. McQuillan, *Chem. Phys. Lett.* 26 (1974) 163.
- [2] D.L. Jeanmaire, R.P. van Duyne, *J. Electroanal. Chem.* 84 (1977) 1.
- [3] E.C. Le Ru, E. Blackie, M. Meyer, P.G. Etchegoin, *J. Phys. Chem. C* 111 (2007) 13794.
- [4] P.G. Etchegoin, E.C. Le Ru, *Phys. Chem. Chem. Phys.* 10 (2008) 6079.
- [5] E.C. Le Ru, E. Blackie, M. Meyer, P.G. Etchegoin, *J. Phys. Chem. B* 110 (2006) 1944.
- [6] J.A. Dieringer, K.L. Wustholz, D.J. Masiello, J.P. Camden, S.L. Kleinman, G.C. Schatz, R.P. van Duyne, *J. Am. Chem. Soc.* 131 (2009) 849.
- [7] K. Kneipp, M. Moskovits, H. Kneipp, *Surface-Enhanced Raman Scattering (Topics in Applied Physics)*, 1st ed., Springer-Verlag Berlin and Heidelberg GmbH & Co. K, 2010.
- [8] S. Nie, S.R. Emory, *Science* 257 (1997) 1102.
- [9] K. Kneipp, Y. Wang, H. Kneipp, L. Perelman, I. Itzkan, R.R. Dasari, M.S. Feld, *Phys. Rev. Lett.* 78 (1997) 1667.
- [10] J. Xie, Q. Zhang, J.Y. Lee, D.I. Wang, *ACS Nano* 2 (2008) 2473.
- [11] Y. Wang, J.L. Seebald, D.P. Szeeto, J. Irudayaraj, *ACS Nano* 4 (2010) 4039.
- [12] J.M. Yuen, N.C. Shah, J.T. Walsh, M.R. Glucksberg, R.P. van Duyne, *Anal. Chem.* 82 (2010) 8382.
- [13] E.C. Le Ru, M. Meyer, P.G. Etchegoin, *J. Phys. Chem. B* 110 (2006) 1944.
- [14] E. Blackie, E.C. Le Ru, M. Meyer, M. Timmer, B. Burkett, P. Northcote, P.G. Etchegoin, *Phys. Chem. Chem. Phys.* 10 (2008) 4147.
- [15] E.C. Le Ru, P.G. Etchegoin, *Principles of Surface-enhanced Raman Spectroscopy and Related Plasmonic Effects*, Elsevier Science, 2008.
- [16] Y. Sawai, B. Takimoto, H. Nabika, K. Ajito, K. Murakoshi, *J. Am. Chem. Soc.* 129 (2007) 1658.
- [17] H. Xu, J. Aizpurua, M. Käll, P. Apell, *Phys. Rev. E* 62 (2000) 4318.
- [18] K. Ueno, S. Juodkazis, T. Shibuya, Y. Yokota, V. Mizeikis, H. Sasaki, H. Misawa, *J. Am. Chem. Soc.* 130 (2008) 6928.
- [19] W.-H. Park, Z.H. Kim, *Nano Lett.* 10 (2010) 4040.
- [20] K. Ikeda, K. Takahashi, T. Masuda, K. Uosaki, *Angew. Chem. Int. Ed.* 50 (2011) 1280.

- [21] B. Lim, H. Kobayashi, T. Yu, J. Wang, M.J. Kim, Z.Y. Li, M. Rycenga, Y. Xia, J. Am. Chem. Soc. 132 (2010) 2507.
- [22] H. Gu, Z. Yang, J. Gao, C.K. Chang, B. Xu, J. Am. Chem. Soc. 127 (2005) 35.
- [23] A.M. Kalsin, A.O. Pinchuk, S.K. Smoukov, M. Paszewski, G.C. Schatz, B.A. Grzybowski, Nano Lett. 6 (2006) 1896.
- [24] C.L. Haynes, R.P. van Duyne, Nano Lett. 3 (2003) 939.
- [25] M. Takase, Y. Sawai, H. Nabika, K. Murakoshi, Trans. Mater. Res. Soc. 32 (2007) 409.
- [26] W.S. Joo, Spectrosc. Lett. 39 (2006) 85.
- [27] W.S. Joo, Vib. Spectrosc. 34 (2004) 269.
- [28] M. Suzuki, Y. Niidome, S. Yamada, Thin Solid Films (2006) 496.
- [29] K. Uosaki, H. Allen, O. Hill, J. Electroanal. Chem. 122 (1981) 321.
- [30] D. Yang, D. Bizzotto, J. Lipkowski, B. Pettinger, S. Mirwald, Phys. Chem. 98 (1994) 7083.
- [31] M.J. Eddowes, H.A.O. Hill, J. Chem. Soc. Chem. Commun. (1977) 3154.
- [32] W.J. Albery, M.J. Eddowes, H.A.O. Hill, A.R. Hillman, J. Am. Chem. Soc. 103 (1981) 3904.
- [33] J.A. Rodriguez, Surf. Sci. 226 (1990) 101.
- [34] D. Mayer, Th. Dretschkow, K. Ataka, Th. Wandlowski, J. Electroanal. Chem. 20 (2002) 524–525.